CONFINE-MAS: a magic-angle spinning NMR probe that confines the sample in case of a rotor explosion

Author(s):
Wiegand, Thomas; Hunkeler, Andreas; Däpp, Alexander; Verasdonck, Joeri; Cadalbert, Riccardo; Bousset, Luc; Melki, Ronald; Böckmann, Anja; Meier, Beat H.

Publication date:
2018-12

Permanent link:
https://doi.org/10.3929/ethz-b-000313278

Originally published in:
Journal of Biomolecular NMR 72(3), https://doi.org/10.1007/s10858-018-0218-x

Funding acknowledgement:
159707 - NMR studies in the Solid State (SNF)
741863 - Faster magic-angle spinning leads to a resolution revolution in biological solid-state NMR (EC)

Journal of Biomolecular NMR (2018) 72:171–177
https://doi.org/10.1007/s10858-018-0218-x

ARTICLE

CONFINE-MAS: a magic-angle spinning NMR probe that confines the sample in case of a rotor explosion

Thomas Wiegand[1] · Andreas Hunkeler[1] · Alexander Däpp[1] · Joeri Verasdonck[1] · Riccardo Cadalbert[1] · Luc Bousset[2] · Ronald Melki[2] · Anja Böckmann[3] · Beat H. Meier[1]

Received: 5 September 2018 / Accepted: 4 December 2018 / Published online: 10 December 2018

Abstract

Magic-angle spinning (MAS) is mandatory in solid-state NMR experiments to achieve resolved spectra. In rare cases, instabilities in the rotation or damage of either the rotor or the rotor cap can lead to a so called "rotor crash" involving a disintegration of the sample container and possibly the release of an aerosol or of dust. We present a modified design of a 3.2 mm probe with a confining chamber which in case of a rotor crash prevents the release of aerosols and possibly hazardous materials. 1D and 2D NMR experiments show that such a hazardous material-confining MAS probe ("CONFINE-MAS" probe) has a similar sensitivity compared to a standard probe and performs equally well in terms of spinning stability. We illustrate the CONFINE-MAS probe properties and performance by application to a fungal amyloid.

Keywords Solid-state NMR · Magic-angle spinning · Safety · Containment

Introduction

Solid-state Nuclear Magnetic Resonance (NMR) is an important method for the characterization of materials and biomolecules. As an example, it is a key method for the characterization of amyloid fibrils in terms of the fast analysis of the polymorphic form or composition, the analysis of the secondary structure, or, more demanding, the determination of the three-dimensional structure (Schütz et al. 2015; Wälti et al. 2016; Tuttle et al. 2016; Wasmer et al. 2008). To obtain spectral resolution, magic-angle sample spinning (MAS), the physical rotation of the sample container (MAS rotor) around an axis inclined by ~ 54.74° with respect to the external magnetic field direction, at rotation frequencies between roughly 10 and 150 kHz is necessary (Andrew et al. 1958; Lowe 1959; Böckmann et al. 2015). Drive and bearing allowing to spin the rotor are provided by pressurized air or nitrogen. The sample containers are most often composed of zirconium oxide with sapphire or boron nitride as alternatives. They have to withstand centrifugal accelerations up to 10^7 g (Böckmann et al. 2015) which sporadically can lead to a catastrophic failure of the container ("rotor crash") with a release of the sample into the air streams used for bearing, drive and cooling of the spinning device. The possible formation of aerosols or dust released to the lab in commercially available magic-angle spinning devices can be an unwanted side effect of such a crash. For hazardous compounds, or such of unknown toxicity, from both fields, materials and biology, this needs to be avoided. In the past, we have used a simple modification of the commercial devices to guide the air into an under-pressured exhaust tube connected to the shim tube from the top of the magnet.

Here, we describe an improved design of a MAS probe with an airtight chamber containing the standard Bruker

Electronic supplementary material The online version of this article (https://doi.org/10.1007/s10858-018-0218-x) contains supplementary material, which is available to authorized users.

✉ Ronald Melki
ronald.melki@cnrs.fr

✉ Anja Böckmann
a.bockmann@ibcp.fr

✉ Beat H. Meier
beme@ethz.ch

[1] Physical Chemistry, ETH Zürich, Vladimir-Prelog-Weg 2, 8093 Zürich, Switzerland

[2] Institut François Jacob, MIRCen, CEA, Laboratory of Neurodegenerative Diseases, CNRS, 18 Rue du Panorama, 92265 Fontenay-aux-Roses, France

[3] Molecular Microbiology and Structural Biochemistry, UMR 5086 CNRS, Université de Lyon, Labex Ecofect, 69367 Lyon, France

3.2 mm spinning device with a controlled exhaust through a HEPA filter. All mechanical, electrical and optical feedthroughs into the chamber are largely airtight, and air connections for bearing, drive and variable temperature are secured by one-way valves. It should however be noted that no significant overpressure is present in the sample chamber during operation, on the contrary it is operated slightly below ambient pressure. The protection chamber can be filled with a solvent or detergent for decontamination if needed (Bousset et al. 2015) before opening the device after a rotor crash. In this phase, the chamber needs to be tight for liquids. The device provides an efficient way to greatly reduce sample material dispersion; it has, however, not been certified for a certain biosafety class.

Probe design, construction, preliminary tests and operation

The central building block of the CONFINE-MAS probe head is an airtight chamber into which all feedthroughs were sealed with O-rings. This chamber replaces the corresponding part of a standard, non "E-free" (Gor'kov et al. 2007), 3.2 mm wide-bore Bruker probe. The bearing air pressure supply and the supply for the cooling gas were equipped with homebuilt back-pressure valves and the drive air pressure supply by a valve that can be manually closed in case of a rotor explosion/crash. A number of modifications was applied to a standard probe. The design of the airtight chamber is shown in form of an exploded view drawing in Fig. 1a

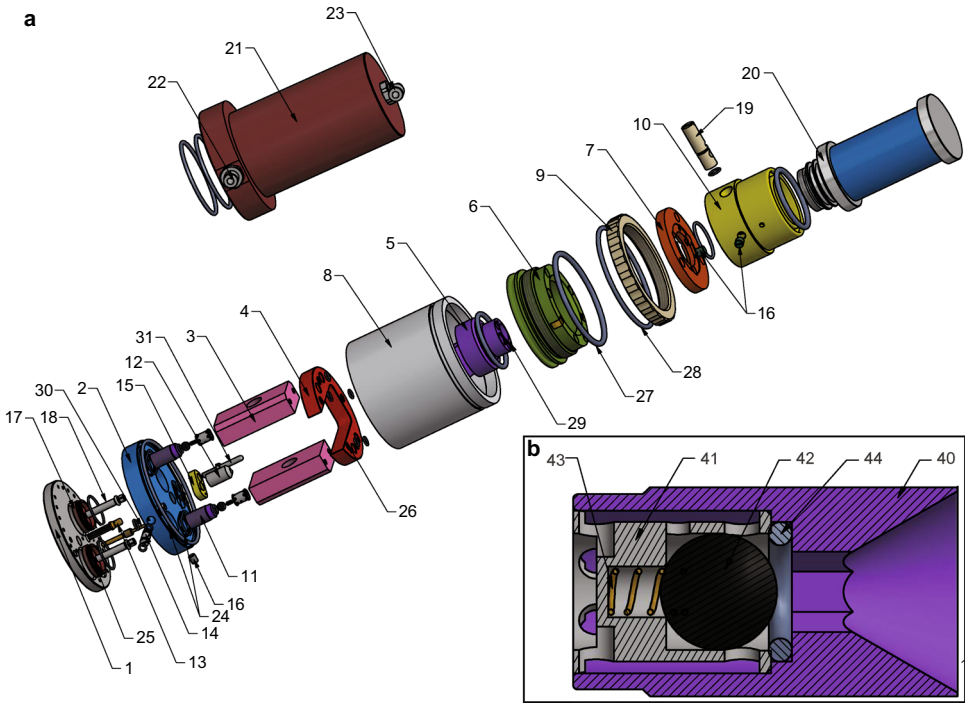

Fig. 1 Design of the 3.2 mm CONFINE-MAS probe. **a** Exploded view drawing of the airtight-chamber added on top of a standard Bruker wide-bore probe. Note that the 3.2 mm stator is missing. **b** Schematic drawing of a back-pressure valve used for the bearing and cooling gas supplies. Asterisk denotes original BRUKER parts

1* Top plate of the existing base frame
2 Probe head bottom
3 Bearing block for 3.2 mm stator
4 Turbine top
5 Insertion channel
6 Exhaust air chamber
7* Fixation ring for insertion channel
8 Temperature control cap
9 Screw collar for exhaust air chamber
10 Filter support
11 Back-pressure valve
12* Mount for optical sensor
13* Optical sensor
14 Cutoff valve for drive air
15 Thrust plate
16 Lock screw
17 High-frequency feedthrough
18* High-frequency line
19 Flushing valve
20 HEPA filter
21 Flushing cap
22 Plug-in connection for pipe (entrance)
23 Plug-in connection for pipe (exit)
24 O-ring groove probe head bottom
25 O-ring groove high-frequency feedthrough
26 O-ring seal turbine top
27 O-ring exhaust air chamber
28 O-ring clamping ring
29 Thread
30 Feedthrough for grounding
31 Rod for MA adjustment
40 Valve frame
41 Ball bearing cage
42 Ceramics ball
43 Bronze spring
44 O-ring check valve

(for the materials used see Table S1). The probe bottom (2) is the central interface between the airtight chamber and the standard probe. 28 continuous boreholes lead through this element out of which 13 were used and had to be sealed with O-rings to obtain an airtight chamber. All O-rings are made out of Nitrile Butadiene Rubber (NBR), except the O-ring between parts (5) and (29), *vide infra* (for further geometric details of the O-rings used see Fig. S1 and Table S2). Figure 2 shows a schematic drawing of this element.

The probe bottom (2) was screwed from the back to the standard probe. O-ring grooves (24) for the temperature control cap (8) and the bearing blocks for the 3.2 mm stator (3) were added. The rod for adjusting the magic angle (31) and the coaxial cables to the thermocouple were sealed by O-rings and a thrust plate (15). We improved the design of this rod to allow for a larger range of angle adjustment. A modified version of high-frequency feedthroughs (17) was built using the more robust material Vespel SP1 instead of

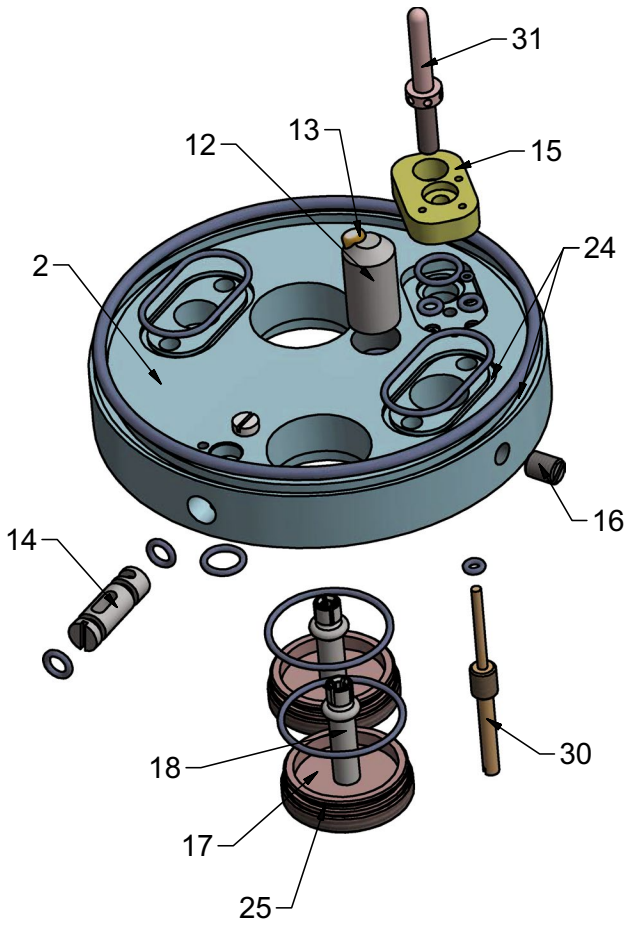

Fig. 2 Sealed feedthroughs are the basis for an airtight chamber. Exploded view drawing of the probe bottom (2) which is the central interface to a standard 3.2 mm probe. All feedthroughs are sealed by O-rings. The nomenclature of the individual elements can be found in Fig. 1

Teflon. They possess an O-ring seal (25) at the outside. The high-frequency line (18) precisely entered this line. The mount for the optical sensor (12) was screwed into the probe bottom and glued with silica. The end cap of the optical sensor required for MAS signal detection (13) was glued with silica in the mount (12). To protect the high-frequency line in case of a rotor crash, the drive air pressure supply was moved to the interior and equipped with a valve that can be closed in case of such an event (14). The two bearing blocks used as supplies for the bearing air pressure and cooling gas were equipped with homebuilt back-pressure valves (11). Such valves consist of light ceramic balls and possess a small opening pressure of around 500 mbar. For more details see below and Fig. 1b for an exploded view drawing. The cap of the turbine (4) was built out of aluminium and is equipped with grooves for the O-rings (26) which seal the screws of the exhaust air chamber (6) that is made out of PEEK and is equipped with an O-ring at the outside to entirely seal the temperature control cap and a screw collar for the clamping ring (9). The clamping ring fixes the temperature control cap and pushes on the seal of the probe bottom. An O-ring at the clamping ring (28) allows for the compensation of any length elongation of the temperature control cap. The insertion channel (5) was adapted from the Bruker design. Only three small exhaust boreholes were sealed and two screws were inserted to fix the filter support (10). The filter support (10) was constructed as connection between the insertion channel (5) and a High Efficiency Particulate Air (HEPA) filter (20). The HEPA filter (20) is a special construction of Donaldson Inc. (Mineapolis, USA) made of non-magnetic material with a filtration efficiency of 99.97% on 0.3 µm particles (First et al. 1998). It can be screwed into the filter support (10). After a rotor crash, the probe is equipped with a flushing cap (21). For that purpose, the filter support is equipped with a flushing valve (19) that closes the insertion channel to the top during flushing and distributes the detergent or other flushing liquid used within the airtight chamber. This allows efficient flushing of the entire probe chamber including the stator. Figure 3a shows a picture of the HEPA filter screwed on top of the probe, as used during measurements. The flushing cap (21) will only be used after a rotor crash, and then covers the complete HEPA filter. The plug-in connections for the flushing pipes (22, 23) were integrated in this cap (see also Fig. 3b).

During construction and preliminary tests, it turned out that the design of the back-pressure valves was critical. In a first version, the required pressure for opening the valve was too high and vibrations were observed leading to an unstable rotation of the MAS rotor. We thus improved the design, in particular by guiding the ceramic ball in the ball bearing cage, and developed the construction shown in Fig. 1b which allows for a stable rotation at 17.0 kHz over several days. Additionally, we realized that a grounding of

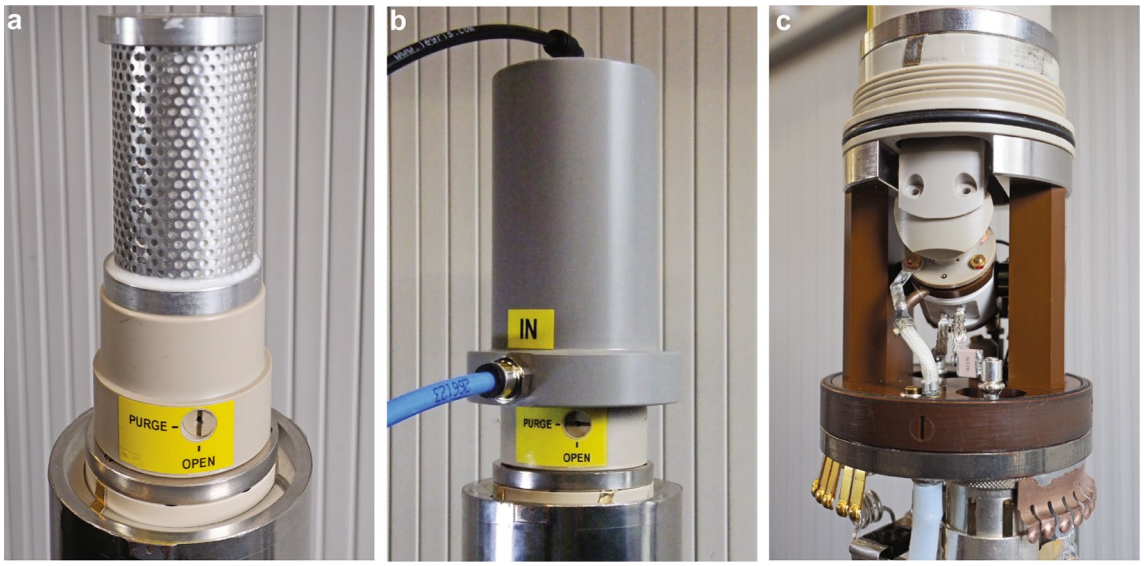

Fig. 3 An airtight chamber on top of a standard 3.2 mm probe. **a** View at the HEPA filter on top of the airtight chamber of the CONFINE-MAS probe. The flushing valve is highlighted in yellow and in the "open" position. The probe is ready for operation in this mode. **b** View at the flushing cap attached to the CONFINE-MAS probe. The flushing valve is in the "purge" position. A flushing of the probe with detergent or other liquid is possible in this configuration. **c** View into the airtight chamber. All feedthroughs to the standard 3.2 mm probe frame at the bottom are sealed

the two thermocouples was required, which was achieved by a grounding pin (30).

Leakage test

The airtight chamber in the assembled probe was tested at 0.3 bar over pressure for a decrease of pressure. During one hour no significant decrease was observed (< 10 mbar).

Operation of the probe

During operation, the shim tube of the magnet is equipped at the top with an additional exhaust tube (see Fig. S2). A slight under pressure (around 200 mbar) is achieved in this tube which guarantees that in the very unlikely case of a release of material from the probe, this is directed into the laboratory exhaust system. This is an additional safety precaution combining the formerly used safety equipment with the CONFINE-MAS probe. As mentioned above, the probe is never operated under overpressure and this test is mainly for detecting possible leaks and to test if it does not leak liquids used for flushing.

Flushing of the probe in case of a rotor explosion

In case of a rotor explosion, the chamber can optionally be flushed with a liquid, e.g. a detergent. The procedure to flush the probe is as follows. The probe will be placed in a fume hood, the shield will be removed and the flushing cap will be attached. The valve for the drive air pressure supply (14) will be closed and the valve at the filter support (10) turned to the position "purge" (see also Fig. 3b) after attaching two pipes for the detergent to flush the probe. One pipe is used to pump the detergent into the chamber (blue in Fig. 3b, e.g., by using a syringe filled with detergent), the other one to collect the solution after the incubation time (black in Fig. 3b). The choice of the detergent as well as the incubation time depends on the material investigated. After flushing the probe several times, the system can be opened and the probe chamber as well as the inlet ports can be cleaned manually. The stator is typically the most contaminated in case of a rotor crash and it may be recommended that it is entirely replaced. Also the HEPA filter should be replaced after a crash. The detergent as well as further contaminated material must be disposed according to the rules for the corresponding hazardous material. We note that a rotor crash already occurred during operation, such that the cleaning procedure described above has already been applied successfully (see also Fig. S3). We believe that this crash was not related to the changed probe design.

Performance

Spinning and sensitivity compared to standard 3.2 probe

Spinning procedures are similar to commercial 3.2 mm probes. However, special care has to be taken when starting the spinning in a MAS experiment in the CONFINE-MAS

probe, since, due to the back-pressure valve, a 500 mbar higher bearing pressure value is required for spinning the rotor up. Typically, we spin the rotor manually up to 8 kHz employing a Bruker MAS II unit and switch to the automatic mode to reach 17 kHz in the end. Once the rotor is spun up, no differences compared to a standard 3.2 mm device in performance and in particular also in spinning stability was observed (the gas pressures applied for bearing and drive for MAS spinning at 17 kHz are the same as for a commercial 3.2 mm probe). Full-width at half maximum (FWHM) of adamantane in a ^{13}C-detected spectrum was ~4 Hz which is comparable to a standard 3.2 mm probe (see Fig. 4 for a comparison of the line shapes obtained) and indicates a reasonable shim for the CONFINE-MAS probe.

The sensitivity of the CONFINE-MAS probe was probed by comparing different standard experiments such as 1D ^{1}H,^{13}C cross-polarization (CPMAS), ^{1}H,^{15}N CPMAS and ^{15}N,^{13}C NCA experiments, recorded on HET-s (218–289) fibrils (Wasmer et al. 2008; Van Melckebeke et al. 2010). The fibrils were washed twice with water before rotor filling and thus contain nearly no salt, therefore mitigating heating effects during radio-frequency pulsing, e.g., high-power ^{1}H decoupling. Figure 5 shows a comparison of 1D ^{1}H,^{13}C cross-polarization (CP MAS) and ^{15}N,^{13}C NCA spectra recorded in the CONFINE-MAS probe (grey) and a standard triple-resonance Bruker 3.2 mm probe (blue). The CP-conditions were optimized in each probe individually. No significant differences in terms of signal-to-noise ratios (SNR, determined on the peak maxima) were observed allowing to conclude that the performance of all three channels is equally well in the CONFINE-MAS probe compared to the standard 3.2 mm probe. For details see Table 1 which includes also matched

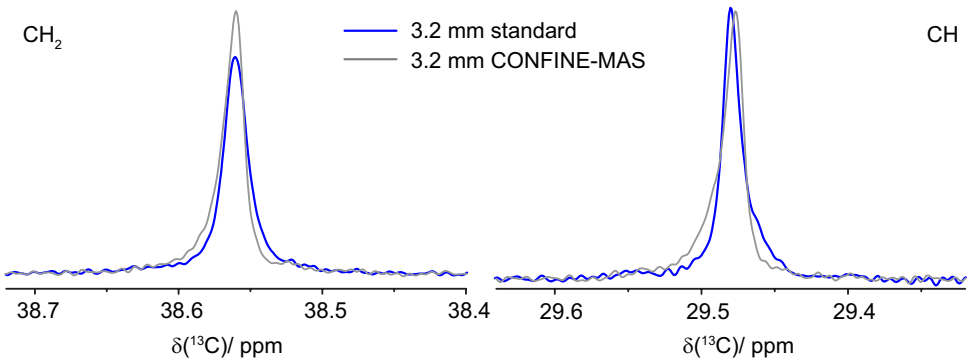

Fig. 4 Narrow ^{13}C lines on adamantane. Comparison of ^{13}C resonances of adamantane used for shimming recorded in the CONFINE-MAS probe (grey) and a standard 3.2 mm probe (blue). A similar FWHM of ~4 Hz was found for both probes

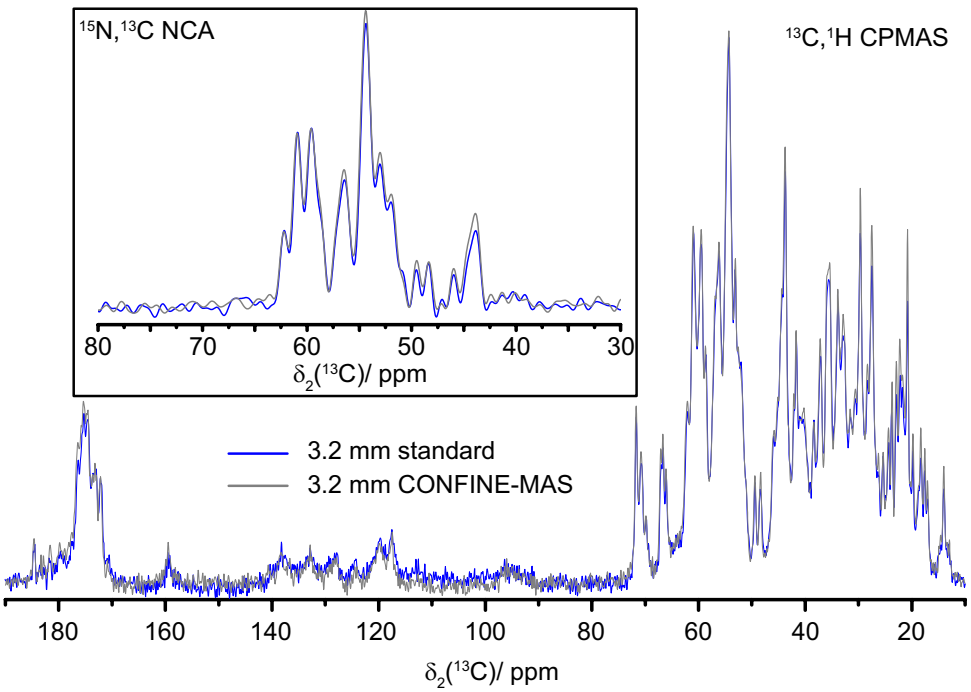

Fig. 5 Similar sensitivity compared to a standard 3.2 mm probe in ^{13}C-detected experiments. Comparison of 1D ^{1}H,^{13}C CPMAS and 1D ^{15}N,^{13}C NCA spectra recorded on a sample of HET-s (218–289) fibrils in a standard 3.2 mm probe (blue) and the CONFINE-MAS probe (grey). All experiments were recorded under similar experimental conditions. The extracted SNR for the corresponding peak maxima are given in Table 1

Table 1 The CONFINE-MAS probe shows a similar performance than a standard 3.2 mm triple resonance probe

	CONFINE-MAS probe	Standard 3.2 mm probe
SNR (^{13}C, ^{1}H CPMAS)	56	55
SNR (^{15}N, ^{1}H CPMAS)	24	18
SNR (^{15}N, ^{13}C NCA)	44	39
SNR (^{13}C–^{13}C DARR)[a]	26	21
SNR (^{15}N–^{13}C NCA)[a]	91	77
Q factor (^{13}C)[b]	127	124
Ball shift (^{13}C)[c]	2.2 MHz	2.4 MHz

Comparison of SNRs for 1D ^{1}H,^{13}C CPMAS, ^{1}H,^{15}N CPMAS, ^{13}C,^{15}N NCA, ^{13}C–^{13}C DARR and ^{15}N–^{13}C NCA spectra determined on a sample of HET-s (218–289) fibrils

[a]Averaged SNR for the ten peaks shown in Fig. 6

[b]The matched Q factor was determined for an empty rotor

[c]The ball shift was assessed for a cylindrical brass perturbation body with the diameter of 2 mm and the length of 2.2 mm

Q-factors determined for an empty rotor and ball shifts which are nearly identical for both probes.

A comparison of 2D ^{13}C–^{13}C Dipolar Assisted Rotational Resonance (DARR) (Takegoshi et al. 1999, 2001) and ^{15}N–^{13}C NCA experiments (Baldus et al. 1998) recorded on HET-s (218–289) fibrils in a standard and in the CONFINE-MAS 3.2 mm probe is shown in Fig. 6. Visually, there is no difference between the spectra measured in the two different probes. The averaged SNR for the ten peaks labeled in red in Fig. 6 are approximately 20% larger for the CONFINE-MAS probe, but this may lie within the variations between setups and individual probes.

Conclusions

The CONFINE-MAS probe described allows for solid-state NMR experiments on hazardous materials, since the release of sample is greatly reduced or avoided in case of a rotor explosion, an event that can never be completely ruled out in MAS experiments. In terms of rf-performance, spinning stability and sensitivity the modified design of the 3.2 mm probe shows no disadvantages compared to a standard probe. In the unfortunate case of a rotor explosion, the probe can be flushed with detergent or other liquids, in which the investigated material (e.g., here protein fibrils) is denatured or the amyloid is dissolved (Bousset et al. 2015). Especially for faster spinning probes in which the probability of a rotor crash increases due to the higher sensitivity towards small fluctuations in air pressure and larger centrifugal accelerations, the use of CONFINE-MAS probes might be even more important.

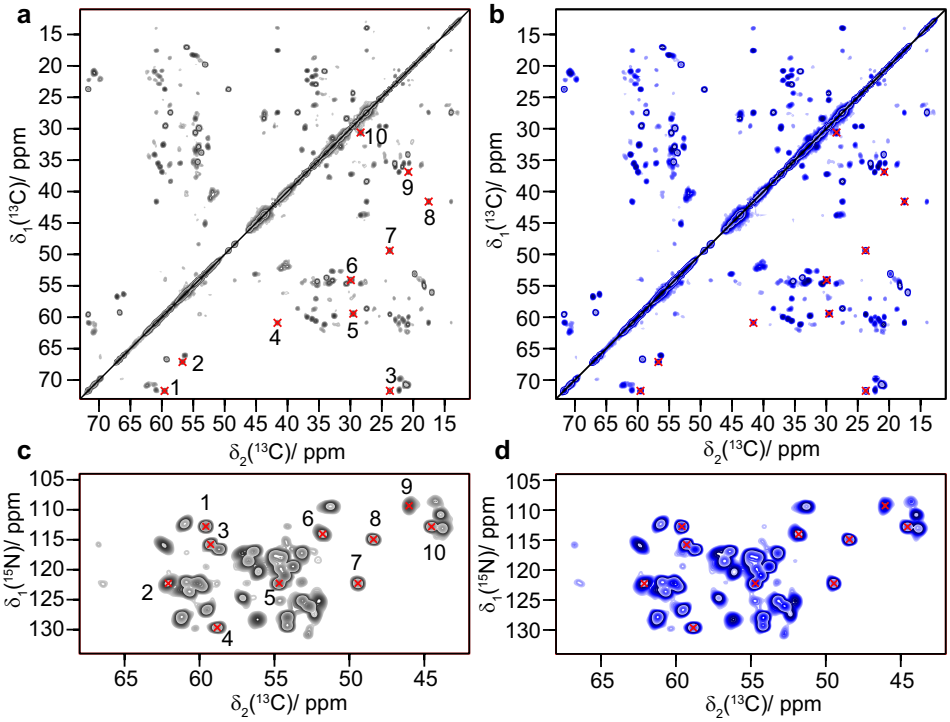

Fig. 6 2D spectra reveal equal performance of the CONFINE-MAS probe and standard 3.2 mm probe. Comparison of ^{13}C–^{13}C DARR spectra (employing a mixing time of 20 ms) and ^{15}N–^{13}C NCA spectra recorded on HET-s (218–289) fibrils in the CONFINE-MAS probe (grey) and a standard 3.2 mm probe (blue). The DARR spectra were plotted at 31 and 28 times noise RMSD for the CONFINE-MAS and standard 3.2 mm probe, respectively, the NCA spectra at 72 and 66 times noise RMSD, respectively. 32 contour levels with an increment of 1.2 are shown. Peaks indicated by red crosses were used for SNR determination (see Table 1). Differences in SNR are attributed to experimental uncertainties and differences in the setups

Materials and methods

Probe construction

The schematic drawings of the airtight chamber were created by using Autodesk inventor. The probe frame is adapted from a standard 3.2 mm Bruker wide bore probe. Construction details are given in Figs. 1, 2, 3 and are described in the main text.

Solid-state NMR

Solid-state NMR experiments were performed at 20.0 T using the CONFINE-MAS probe and a standard 3.2 mm triple-resonance probe. HET-s (218–289) fibrils were prepared according to reference (Van Melckebeke et al. 2010). The MAS frequency was set to 17.0 kHz. Typical CP-conditions for all experiments described herein were $\omega(^{1}H) = 60$ kHz, $\omega(^{13}C) = 46$–47 kHz and $\omega(^{15}N) = 45$ kHz for $^{1}H,^{13}C$ and $^{1}H,^{15}N$ CP and $\omega(^{13}C) = 6$ kHz and $\omega(^{15}N) = 11$ kHz for SPECIFIC NCA experiments. 90 kHz SPINAL-64 ^{1}H decoupling was applied during evolution and detection. Typical acquisition times in the direct dimension were 15.4 ms and in the indirect dimension 11.5–12.8 ms for all HET-s spectra. For adamantane, 5 kHz WALTZ-64 ^{1}H decoupling was applied and the acquisition time was set to 655 ms. The 2D spectra were processed with the software TOPSPIN (version 3.5, Bruker Biospin) with a shifted (3.0) squared cosine apodization function and automated baseline correction in the indirect and direct dimensions. The sample temperature was set to 283 K (Böckmann et al. 2009). All spectra were analysed with the software CcpNmr (Fogh et al. 2002; Vranken et al. 2005; Stevens et al. 2011) and referenced to 4,4-dimethyl-4-silapentane-1-sulfonic acid (DSS). SNRs were determined using the implemented routine in TOPSPIN for the 1D spectra and with CcpNMR for the 2D spectra (in the latter case the RMSD noise level was taken from TOPSPIN).

Acknowledgements This work was supported by the Swiss National Science Foundation (Grant 200020_159707), by the French ANR (ANR-11-LABX-0048 through ANR-11-IDEX-0007), and the ETH Career SEED-69 16-1. This project has received funding from the European Research Council (ERC) under the European Union's Horizon 2020 research and innovation programme (Grant agreement no. 741863, FASTER).

References

Andrew ER, Bradbury A, Eades RG (1958) Nuclear magnetic resonance spectra from a crystal rotated at high speed. Nature 182:1659–1659

Baldus M, Petkova AT, Herzfeld J, Griffin RG (1998) Cross polarization in the tilted frame: assignment and spectral simplification in heteronuclear spin systems. Mol Phys 95:1197–1207

Böckmann A et al (2009) Characterization of different water pools in solid-state NMR protein samples. J Biomol NMR 45:319–327

Böckmann A, Ernst M, Meier BH (2015) Spinning proteins, the faster, the better? J Magn Reson 253:71–79

Bousset L, Brundin P, Böckmann A, Meier B, Melki R (2015) An efficient procedure for removal and inactivation of alpha-synuclein assemblies from laboratory materials. J Parkinson's Dis 6:143–151

First MW (1998) HEPA filters. J Am Biol Saf Assoc 3:33–42

Fogh R et al (2002) The CCPN project: an interim report on a data model for the NMR community. Nat Struct Mol Biol 9:416–418

Gor'kov PL et al (2007) Low-E probe for 19F–1H NMR of dilute biological solids. J Magn Reson 189:182–189

Lowe IJ (1959) Free induction decays of rotating solids. Phys Rev Lett 2:285–287

Schütz AK et al (2015) Atomic-resolution three-dimensional structure of amyloid β fibrils bearing the Osaka mutation. Angew Chem Int Ed 54:331–335

Stevens T et al (2011) A software framework for analysing solid-state MAS NMR data. J Biomol NMR 51:437–447

Takegoshi K, Nakamura S, Terao T (1999) 13C–13C polarization transfer by resonant interference recoupling under magic-angle spinning in solid-state NMR. Chem Phys Lett 307:295–302

Takegoshi K, Nakamura S, Terao T (2001) 13C–1H dipolar-assisted rotational resonance in magic-angle spinning NMR. Chem Phys Lett 344:631–637

Tuttle MD et al (2016) Solid-state NMR structure of a pathogenic fibril of full-length human α-synuclein. Nat Struct Mol Biol 23:409

Van Melckebeke H et al (2010) Atomic-resolution three-dimensional structure of HET-s (218–289) amyloid fibrils by solid-state NMR spectroscopy. J Am Chem Soc 132:13765–13775

Vranken WF et al (2005) The CCPN data model for NMR spectroscopy: development of a software pipeline. Proteins 59:687–696

Wälti MA et al (2016) Atomic-resolution structure of a disease-relevant Aβ(1–42) amyloid fibril. Proc Natl Acad Sci USA 113:E4976–E4984

Wasmer C et al (2008) Amyloid fibrils of the HET-s (218–289) prion form a β solenoid with a triangular hydrophobic core. Science 319:1523–1526